

A non-invasive, reference region-based method for quantification of cerebral blood flow and oxygen metabolism using oxygen-15 labeled gases and positron emission tomography

Hiroshi Ito ^{1,2*†}, Masanobu Ibaraki ^{3†}, Ryo Yamakuni ¹, Naoyuki Ukon ², Shiro Ishii ¹, Kenji Fukushima ¹, Hitoshi Kubo ^{2,4}, Kazuhiro Takahashi ²

¹Department of Radiology and Nuclear Medicine, Fukushima Medical University, Fukushima, Japan

²Advanced Clinical Research Center, Fukushima Medical University, Fukushima, Japan

³Department of Radiology and Nuclear Medicine, Akita Research Institute of Brain and Blood Vessels, Akita, Japan

⁴Department of Radiological Sciences, School of Health Sciences, Fukushima Medical University, Fukushima, Japan

ARTICLE INFO

Article type:
Original Article

Article history:

Received: 26 Jul 2024

Revised: 17 Jan 2025

Accepted: 25 Mar 2025

Keywords:

Brain

CBF

CMRO₂

OEF

PET

ABSTRACT

Objective(s): Measurement of cerebral blood flow (CBF), cerebral blood volume (CBV), cerebral oxygen extraction fraction (OEF), and cerebral metabolic rate of oxygen (CMRO₂) by positron emission tomography (PET) with oxygen-15 labeled gases is widely used for investigation into the pathophysiology of occlusive cerebrovascular disease. However, all methods for quantification of CBF, CBV, OEF, and CMRO₂ by PET with oxygen-15 labeled gases require invasive arterial blood sampling. The present study developed a reference region-based method for quantification of CBF, CBV, OEF, and CMRO₂ using PET and oxygen-15 labeled gases based on the steady-state method without invasive arterial blood sampling.

Methods: The CBF, CBV, OEF, and CMRO₂ were measured in patients with occlusive cerebrovascular disease by PET using ¹⁵O-labeled gases, C¹⁵O₂, C¹⁵O, and ¹⁵O₂, with the steady-state method. In the present method, the ratios of values in a brain region to the reference region for CBF, CBV, OEF, and CMRO₂ were calculated without invasive arterial blood sampling.

Results: Good correlations were observed for the ratios of values of the cerebral lesion to the reference brain region for CBF, CBV, OEF, and CMRO₂ calculated by the present method as compared with those obtained by the steady-state method with arterial blood sampling, indicating its validity. Simulation studies showed that errors in estimated values calculated by the present method were negligibly small for both conditions of misery perfusion and matched hypoperfusion.

Conclusion: A simple method for noninvasive quantification of CBF, CBV, OEF, and CMRO₂ using PET and oxygen-15 labeled gases could be developed based on the steady-state method. This method can be used to investigate the pathophysiology of occlusive cerebrovascular disease.

► Please cite this paper as:

Ito H, Ibaraki M, Yamakuni R, Ukon N, Ishii Sh, Fukushima K, Kubo H, Takahashi K. A non-invasive, reference region-based method for quantification of cerebral blood flow and oxygen metabolism using oxygen-15 labeled gases and positron emission tomography. *Asia Ocean J Nucl Med Biol.* 2025; 13(2): 126-137. doi: 10.22038/aojnmb.2025.81433.1578

Introduction

Measurement of cerebral blood flow (CBF), cerebral blood volume (CBV), cerebral oxygen extraction fraction (OEF), and cerebral metabolic rate of oxygen (CMRO₂) by positron emission tomography (PET) with ¹⁵O-labeled

carbon dioxide (C¹⁵O₂), ¹⁵O-labeled carbon monoxide (C¹⁵O), or ¹⁵O-labeled oxygen (¹⁵O₂) is widely used for investigation into the pathophysiology of several brain diseases, especially occlusive cerebrovascular disease (1-8). Decreased cerebral perfusion pressure due

* Corresponding author: Hiroshi Ito. Department of Radiology and Nuclear Medicine, Fukushima Medical University, 1 Hikariga-oka, Fukushima 960-1295, Japan. Tel: (+81) 24-547-1334; Fax: (+81) 24-549-3789; E-mail: h-ito@fmu.ac.jp

† Hiroshi Ito and Masanobu Ibaraki contributed equally to this work.

© 2025 *mums.ac.ir* All rights reserved.

This is an Open Access article distributed under the terms of the Creative Commons Attribution License (<http://creativecommons.org/licenses/by/3.0>), which permits unrestricted use, distribution, and reproduction in any medium, provided the original work is properly cited.

to major cerebral arterial occlusive disease causes cerebral autoregulatory vasodilatation to maintain CBF (stage I hemodynamic change).

Decreased cerebral perfusion pressure below the lower limit of cerebral autoregulation causes a decrease in CBF with an increase in OEF for maintenance of CMRO₂ (stage II hemodynamic change). Although clinical assessment of stage II hemodynamic changes is widely performed using the more popular modality of single photon emission tomography (SPECT) to measure resting and acetazolamide-loaded CBF (9, 10), ¹⁵O-gas PET, which can directly detect elevated OEF, a specific hemodynamic index in stage II, is the most accurate and helpful modality (11).

A significant problem with quantitative ¹⁵O-gas PET performed with various acquisition protocols is the need for invasive arterial blood sampling to measure arterial input function (AIF). While the risk of this blood sampling procedure in PET is not high (12), it is a barrier to widespread clinical use, especially with integrated PET/MRI systems, where the blood sampling procedure is complicated during the examination. Several ¹⁵O-gas PET studies have proposed methods to non-invasively estimate AIF: image-derived input function (IDIF), simultaneous estimation of the input function (SIME), and a combination of these methods (13-16). However, these non-invasive AIF estimation methods involve advanced, complicated image processing and mathematical modeling of dynamic PET images, making them impractical for clinical use and challenging to apply to the most widely used ¹⁵O-gas PET examination protocol, the steady-state method (17,18).

On the other hand, as an alternative method that is simpler and applicable to the steady-state method, several authors have proposed non-invasive ¹⁵O-gas PET using the so-called reference region method based on the steady-state method and other acquisition methods (19-21), which calculates relative values of each hemodynamic parameter to a user-defined reference region instead of calculating absolute values. These reference region-based methods can detect elevated relative OEF values in the ipsilateral hemisphere, a specific feature of stage II hemodynamic changes in patients with occlusive cerebrovascular disease. However, these existing methods do not perform the blood volume correction usually required for quantitative ¹⁵O-gas PET (19) or only perform simple correction using CBV assumptions or pre-determined adjustment parameters (20, 21). Thus, with the existing methods, the reference region-based relative OEF estimates

inevitably include errors due to CBV, which is a problem considering CBV is much higher in the ipsilateral hemisphere with stage II.

This study proposes a non-invasive, clinically realistic method for measuring relative values of CBF, CBV, OEF, and CMRO₂ by ¹⁵O-gas PET with the SS protocol. The proposed method extends the reference region-based method we developed for ¹⁵O-PET with the short inhalation protocol (20) to the steady-state method protocol. It also applies direct vascular component correction using C¹⁵O images to improve the accuracy of OEF estimation. To demonstrate the clinical applicability of this method, we conducted a direct comparison with the results of conventional quantitative analysis using the blood sampling data in patients with steno-occlusive lesions of major cerebral arteries (n=8) performed on an integrated PET/MRI scanner. The proposed method is a reference region-based method; it is necessary to define a reference region in a normal hemodynamic condition in advance and set values for each hemodynamic parameter, CBF, CBV, and OEF in the reference region. Therefore, the discrepancy between these assumed values and the actual values in each patient is an error source for each parameter map; the degree of error was evaluated by computer simulation assuming some hemodynamic scenarios.

Methods

Theory

The theory of the present method for quantification of CBF, CBV, OEF, and CMRO₂ using PET and oxygen-15 labeled gases without an arterial blood sampling based on the steady-state method (see appendix) (17, 18, 22) is as follows. CBF, CBV, OEF, and CMRO₂ in a brain region are defined as CBF_i , CBV_i , OEF_i , and $CMRO_{2i}$, respectively. CBF, CBV, OEF, and CMRO₂ in the reference brain region are defined as CBF_{Ref} , CBV_{Ref} , OEF_{Ref} , and $CMRO_{2Ref}$, respectively. The radioactivity concentrations in the brain and blood are defined as follows:

$C_i^{CO_2}$: Radioactivity concentration of H₂¹⁵O in a brain region measured by PET during inhalation of C¹⁵O₂ gas after equilibrium had been reached

C_i^{CO} : Radioactivity concentration of hemoglobin (Hb)C¹⁵O in a brain region measured by PET after inhalation of C¹⁵O gas

$C_i^{O_2}$: Radioactivity concentration in a brain region measured by PET during inhalation of ¹⁵O₂ gas after equilibrium had been reached

$C_{Ref}^{CO_2}$: Radioactivity concentration of H₂¹⁵O in the reference brain region measured by PET during inhalation of C¹⁵O₂ gas after equilibrium

had been reached

C_{Ref}^{CO} : Radioactivity concentration of HbC¹⁵O in the reference brain region measured by PET after inhalation of C¹⁵O gas

C_{Ref}^{O2} : Radioactivity concentration in the reference brain region measured by PET during inhalation of ¹⁵O₂ gas after equilibrium had been reached

C_a^{CO2} : Radioactivity concentration of H₂¹⁵O in whole blood during inhalation of C¹⁵O₂ gas after equilibrium had been reached

C_p^{CO2} : Radioactivity concentration of H₂¹⁵O in plasma during inhalation of C¹⁵O₂ gas after equilibrium had been reached

C_a^{CO} : Radioactivity concentration of HbC¹⁵O in whole blood after inhalation of C¹⁵O gas

C_a^{O2} : Radioactivity concentration in whole blood during inhalation of ¹⁵O₂ gas after equilibrium had been reached

$C_{a[0]}^{O2}$: Radioactivity concentration of Hb¹⁵O₂ in whole blood during inhalation of ¹⁵O₂ gas after equilibrium had been reached

$C_{a[w]}^{O2}$: Radioactivity concentration of H₂¹⁵O in whole blood during inhalation of ¹⁵O₂ gas after equilibrium had been reached

$C_{p[w]}^{O2}$: Radioactivity concentration of H₂¹⁵O in plasma during inhalation of ¹⁵O₂ gas after equilibrium had been reached

The ratios of values in a brain region to the reference region for CBF, CBV, OEF, and CMRO₂ are defined as $RCBF_i$, $RCBV_i$, $ROEF_i$, and $RCMRO_{2i}$, respectively as follows:

$$RCBF_i = \frac{CBF_i}{CBF_{Ref}} \tag{Eq. 1}$$

$$RCBV_i = \frac{CBV_i}{CBV_{Ref}} \tag{Eq. 2}$$

$$ROEF_i = \frac{OEF_i}{OEF_{Ref}} \tag{Eq. 3}$$

$$RCMRO_{2i} = \frac{CMRO_{2i}}{CMRO_{2Ref}} \tag{Eq. 4}$$

In the present method, $RCBF_i$, $RCBV_i$, $ROEF_i$, and $RCMRO_{2i}$ were calculated without invasive arterial blood sampling. The flowchart for calculation of $RCBF_i$, $RCBV_i$, $ROEF_i$, and $RCMRO_{2i}$, is shown in Figure 1. From radioactivity concentrations in a brain region and the reference brain region measured by PET with C¹⁵O₂, C¹⁵O, and ¹⁵O₂ gases (C_i^{CO2} , C_i^{CO} , C_i^{O2} , C_{Ref}^{CO2} , C_{Ref}^{CO} , C_{Ref}^{O2} , respectively), and assumed values of CBF, CBV, OEF, and CMRO₂ in the reference brain region (CBF_{Ref} , CBV_{Ref} , OEF_{Ref} , and $CMRO_{2Ref}$, respectively), $RCBF_i$, $RCBV_i$, $ROEF_i$, and $RCMRO_{2i}$ are calculated.

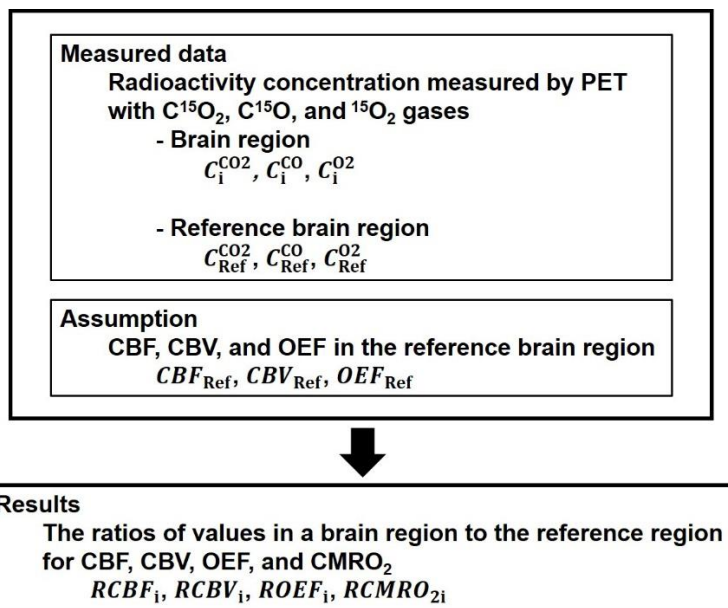


Figure 1. The flowchart for calculation of the ratios of values in a brain region to the reference region for CBF, CBV, OEF, and CMRO₂ ($RCBF_i$, $RCBV_i$, $ROEF_i$, and $RCMRO_{2i}$, respectively). From radioactivity concentrations in a brain region and the reference brain region measured by PET with C¹⁵O₂, C¹⁵O, and ¹⁵O₂ gases (C_i^{CO2} , C_i^{CO} , C_i^{O2} , C_{Ref}^{CO2} , C_{Ref}^{CO} , C_{Ref}^{O2} , respectively), and assumed values of CBF, CBV, OEF, and CMRO₂ in the reference brain region (CBF_{Ref} , CBV_{Ref} , OEF_{Ref} , and $CMRO_{2Ref}$, respectively), $RCBF_i$, $RCBV_i$, $ROEF_i$, and $RCMRO_{2i}$ are calculated

1 .Calculation of RCBF_i

The following equations are derived from Eq. A2:

$$C_{\text{Ref}}^{\text{CO}_2} = C_a^{\text{CO}_2} \cdot \frac{CBF_{\text{Ref}}}{\frac{CBF_{\text{Ref}}}{p} + \lambda} \quad \text{Eq. 5}$$

Where p is the brain-blood partition coefficient, which can be assumed to be unity. λ is the decay constant of ^{15}O . When CBF_{Ref} is assumed, $C_a^{\text{CO}_2}$ can be calculated. The following equations are derived from Eq. A3:

$$CBF_i = \frac{\lambda}{\frac{C_a^{\text{CO}_2}}{C_i^{\text{CO}_2}} - \frac{1}{p}} \quad \text{Eq. 6}$$

Substituting $C_a^{\text{CO}_2}$ into Eq. 6 yields CBF_i for $C_i^{\text{CO}_2}$, and Eq. 1 yields $RCBF_i$.

2 .Calculation of RCBV_i

The following equations are derived from Eq. A4:

$$C_{\text{Ref}}^{\text{CO}} = C_a^{\text{CO}} \cdot CBV_{\text{Ref}} \cdot \frac{h}{H} \quad \text{Eq. 7}$$

Where h and H are hematocrits in the cerebral and large vessels, respectively. The hematocrit ratio of cerebral to large vessels, $h/(H)$, can be assumed to be 0.85 (18, 23, 24). When CBV_{Ref} is assumed, C_a^{CO} can be calculated. The following equations are derived from Eq. A5:

$$CBV_i = \frac{C_i^{\text{CO}}}{C_a^{\text{CO}}} \cdot \frac{H}{h} \quad \text{Eq. 8}$$

Substituting C_a^{CO} into Eq. 8 yields CBV_i for C_i^{CO} , and Eq. 2 yields $RCBV_i$.

3 .Calculation of ROEF_i

The following equations are derived from Eq. A9:

$$OEF'_i = \frac{C_a^{\text{CO}_2}}{C_{a[\text{O}]}^{\text{CO}_2}} \cdot \left(\frac{C_i^{\text{O}_2}}{C_i^{\text{CO}_2}} - \frac{C_{a[\text{w}]}^{\text{O}_2}}{C_a^{\text{CO}_2}} \right) = \frac{C_i^{\text{O}_2}}{C_{a[\text{O}]}^{\text{CO}_2}} - R_m \quad \text{Eq. 9}$$

Or

$$C_i^{\text{O}_2} = C_{a[\text{O}]}^{\text{O}_2} \cdot \frac{C_i^{\text{CO}_2}}{C_a^{\text{CO}_2}} \cdot (OEF'_i + R_m) \quad \text{Eq. 9'}$$

Where

$$R_m = \frac{C_{a[\text{w}]}^{\text{O}_2}}{C_{a[\text{O}]}^{\text{O}_2}} \quad \text{Eq. 10}$$

R_m can be assumed to be 0.214 (25). OEF'_i is cerebral oxygen extraction fraction without correction of remaining radioactivity concentration of $^{15}\text{O}_2$ in the cerebral vessels (26, 27). The relation between OEF'_i and cerebral oxygen extraction fraction with correction of

remaining radioactivity concentration of $^{15}\text{O}_2$ in the cerebral vessels, OEF'_i , can be expressed as follows (Eq. A13):

$$OEF'_i = OEF_i \cdot (1 - X_i) + X_i \quad \text{Eq. 11}$$

Or

$$OEF_i = \frac{OEF'_i - X_i}{1 - X_i} \quad \text{Eq. 11'}$$

Where (Eq. A14)

$$X_i = \frac{\frac{CBF_i}{p} + \lambda}{\frac{h}{H}CBV_i + \lambda} \quad \text{Eq. 12}$$

The following equations are derived from Eq. 9', 11, and 12:

$$C_{\text{Ref}}^{\text{O}_2} = C_{a[\text{O}]}^{\text{O}_2} \cdot \frac{C_{\text{Ref}}^{\text{CO}_2}}{C_a^{\text{CO}_2}} \cdot (OEF'_{\text{Ref}} + R_m) \quad \text{Eq. 13}$$

$$OEF'_{\text{Ref}} = OEF_{\text{Ref}} \cdot (1 - X_{\text{Ref}}) + X_{\text{Ref}} \quad \text{Eq. 14}$$

$$X_{\text{Ref}} = \frac{\frac{CBF_{\text{Ref}}}{p} + \lambda}{\frac{h}{H}CBV_{\text{Ref}} + \lambda} \quad \text{Eq. 15}$$

When OEF_{Ref} is assumed, $C_{a[\text{O}]}^{\text{O}_2}$ can be calculated using CBF_{Ref} , CBV_{Ref} , $C_{\text{Ref}}^{\text{CO}_2}$, $C_{\text{Ref}}^{\text{O}_2}$, and $C_a^{\text{CO}_2}$. OEF_i can be calculated from Eq. 9, 11', and 12, and Eq. 3 yields $ROEF_i$.

4 .Calculation of RCMRO_{2i}

The following equations are derived from Eq. A15:

$$CMRO_{2i} = OEF_i \cdot CBF_i \cdot [O_2] \quad \text{Eq. 16}$$

$$CMRO_{2\text{Ref}} = OEF_{\text{Ref}} \cdot CBF_{\text{Ref}} \cdot [O_2] \quad \text{Eq. 17}$$

Where $[O_2]$ is the total oxygen content in arterial blood. The following equation is derived from Eq. 4, 16, and 17.

$$RCMRO_{2i} = \frac{CMRO_{2i}}{CMRO_{2\text{Ref}}} = \frac{OEF_i \cdot CBF_i}{OEF_{\text{Ref}} \cdot CBF_{\text{Ref}}} \quad \text{Eq. 18}$$

$RCMRO_{2i}$ can be calculated using CBF_i , OEF_i , CBF_{Ref} , and OEF_{Ref} .

In the present method, CBF_{Ref} , CBV_{Ref} , and OEF_{Ref} were assumed to be 0.3 mL/mL/min, 0.03 mL/mL, and 0.4, respectively (22).

Subjects

This study is a retrospective analysis of consecutive PET examinations using oxygen-15 labeled gases performed on eight patients with

steno-occlusive lesions of major cerebral arteries (49-67 years of age; 5 males and 3 females; 1 internal carotid artery stenosis, 3 middle cerebral artery stenosis, 4 middle cerebral artery occlusion) between April 2018 and December 2022. The study was approved by the Institutional Review Board of Fukushima Medical University, Fukushima, Japan.

PET Experimental Procedure

All PET studies were performed with a Siemens mMR PET/MRI scanner, which provides 127 sections with an axial field of view of 25.8 cm (28). The intrinsic spatial resolution was 4.3 mm full-width at half maximum (FWHM) in-plane and 4.3 mm FWHM axially.

Data were acquired in three-dimensional mode. Scatter was corrected (29). PET measurements with the steady-state method of ^{15}O -labeled gases, C^{15}O , $^{15}\text{O}_2$, and C^{15}O_2 were performed on all subjects (17, 18, 22). Static PET scanning was started 3 min after 1 min of continuous inhalation of C^{15}O gas (a total of approximately 3 GBq supplied by mouth). The scanning time was 4 min. Then, static PET scanning was performed during inhalation of $^{15}\text{O}_2$ gas after equilibrium had been reached and confirmed by the head radioactivity curve (a total of approximately 8.4 GBq supplied by mouth). The scanning time was 10 min, and the time from the beginning of inhalation to the beginning of scanning was 10 min. Static PET scanning was performed during inhalation of C^{15}O_2 gas using the same protocol as that used with $^{15}\text{O}_2$ gas (a total of approximately 2.8 GBq supplied by mouth). During each PET scanning, arterial blood sampling was performed to measure the radioactivity concentration in the blood and plasma. Arterial blood gases were also measured. Total oxygen content in arterial blood was estimated from P_aO_2 , pH, and hemoglobin (Hb) concentration (18, 30). PET image reconstruction was carried out by the ordered-subset expectation maximization (OSEM) algorithm (iterations: 3, subsets: 21) with a post-reconstruction Gaussian filter of 5 mm FWHM. Using reconstructed PET images, the radioactivity concentration in arterial blood and plasma, and arterial blood gases data, the parametric images of CBF, CBV, OEF, and CMRO_2 were calculated (See appendix) (17).

All MRI studies were performed with a Siemens mMR PET/MRI scanner, equipped with a 3.0-T MR scanner, during and between PET scanning. Dixon sequence (DIXON) (3D-VIBE (volumetric interpolated breath-hold examination), TR: 3.56 ms, TE: 1.23 ms and 2.46 ms; field of view: 500 mm, slice thickness: 3.12 mm, resolution: $2.6 \times 2.6 \times 3.1$ mm, 1 slab: 128

slices) was performed for attenuation correction of PET (31). Three-dimensional volumetric T1-weighted images (T1WI) and T2-weighted images (T2WI), diffusion-tensor images, arterial spin labeling images, and MR angiography were also acquired.

Data analysis

Regions of interest (ROIs) were drawn on all PET images, referring to T1WI and T2WI. Circular ROIs (10 mm in diameter) were defined for the area of lesion in the cerebrum, excluding cerebral infarction. ROIs were also defined for the contralateral side of the cerebral lesion and the ipsilateral cerebellar cortex of the cerebral lesion. The ipsilateral cerebellar cortex of the cerebral lesion was used as the reference brain region. The ratio of CBF, CBV, OEF, and CMRO_2 with arterial blood sampling based on the steady-state method in the cerebral lesion and its contralateral side to those in the reference brain region were calculated. These values were compared with RCBF_i , RCBV_i , ROEF_i and RCMRO_{2i} , calculated by the present method.

Simulation studies

Simulation studies were performed to estimate systematic errors of RCBF_i , ROEF_i , and RCMRO_{2i} calculated by the present method when CBF in the reference brain region, CBF_{Ref} , deviates from the assumed value. The assumed values of CBF_{Ref} , CBV_{Ref} , and OEF_{Ref} were 0.3 mL/mL/min, 0.03 mL/mL, and 0.4, respectively. CBF_{Ref} was varied in five steps from -30% to +30% from the assumed value. CBV_{Ref} and OEF_{Ref} were also varied so that CBV_{Ref} divided by CBF_{Ref} , corresponding to vascular mean transit time, and CBF_{Ref} multiplied by OEF_{Ref} , corresponding to $\text{CMRO}_{2\text{Ref}}$, were constant.

Errors of RCBF_i

CBF often decreases in occlusive cerebrovascular diseases. Thus, the systematic error of RCBF_i was estimated when RCBF_i varied from 0.2 to 1.0. RCBF_i values were estimated using radioactivity concentrations in a brain region and the reference brain region, which were calculated according to the assumptions. The estimated RCBF_i values were compared to the assumed RCBF_i values.

Errors of ROEF_i

The stage II hemodynamic change in occlusive cerebrovascular diseases due to decreased cerebral perfusion pressure below the lower limit of cerebral autoregulation shows a decrease in CBF with an increase in OEF for maintenance of CMRO_2 , so-called "misery

perfusion" (2). Thus, the systematic error of $ROEF_i$ was estimated when $ROEF_i$ varied from 1.0 to 2.0. In this simulation, CBF_i and OEF_i were varied so that CBF_i multiplied by OEF_i , corresponding to $CMRO_{2i}$, were constant. Since the stage II hemodynamic change also shows an increase in CBV (2), $RCBV_i$ was varied to 1.0, 1.5, and 2.0. $ROEF_i$ values were estimated using radioactivity concentrations in a brain region and the reference brain region, which were calculated according to the assumptions. The estimated $ROEF_i$ values were compared to the assumed $ROEF_i$ values.

Errors of $RCMRO_{2i}$

Oxygen hypometabolism with hypoperfusion in occlusive cerebrovascular diseases can be observed in lesions with neural damage, so called "matched hypoperfusion" (32). Thus, the systematic error of $RCMRO_{2i}$ was estimated when $RCMRO_{2i}$ varied from 0.2 to 1.0. CBF_i and

$CMRO_{2i}$ were varied so that $ROEF_i$ and $RCBV_i$ divided by $RCBF_i$, corresponding to vascular mean transit time, were unity (33). $RCMRO_{2i}$ values were estimated using radioactivity concentrations in a brain region and the reference brain region, which were calculated according to the assumptions. The estimated $RCMRO_{2i}$ values were compared to the assumed $RCMRO_{2i}$ values.

Results

Figure 2 shows typical PET images of CBF_i , CBV_i , OEF_i , and $CMRO_{2i}$ obtained by the steady-state method with arterial blood sampling and corresponding PET images of $RCBF_i$, $RCBV_i$, $ROEF_i$, and $RCMRO_{2i}$ calculated by the present method for a patient with left middle cerebral artery occlusion. Similar regional distributions were observed between them.

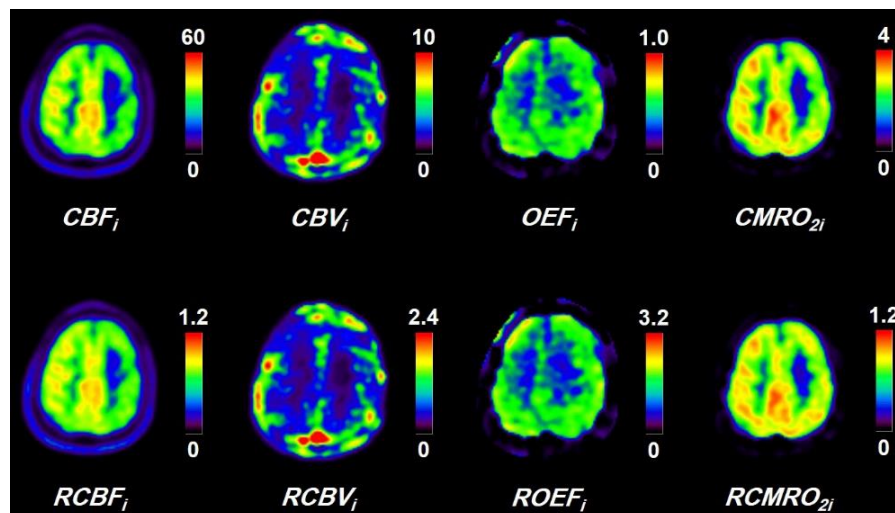


Figure 2. Typical PET images of CBF_i , CBV_i , OEF_i , and $CMRO_{2i}$ obtained by the steady-state method with arterial blood sampling and corresponding PET images of $RCBF_i$, $RCBV_i$, $ROEF_i$, and $RCMRO_{2i}$ calculated by the present method for a patient with left middle cerebral artery occlusion. Scale maximum values are 60 mL/100 mL/min, 10 mL/100 mL, 1.0, and 4 mL/100 mL/min for CBF_i , CBV_i , OEF_i , and $CMRO_{2i}$ images, respectively

The relation between the ratio of CBF_i to CBF_{Ref} obtained by the steady-state method with arterial blood sampling and $RCBF_i$ calculated by the present method for both the cerebral lesion and the contralateral side of the

cerebral lesion is shown in Figure 3A. Such relations for $RCBV_i$, $ROEF_i$ and $RCMRO_{2i}$ are also demonstrated in Figure 3B, 3C, and 3D, respectively. Good correlations were observed for all relations.

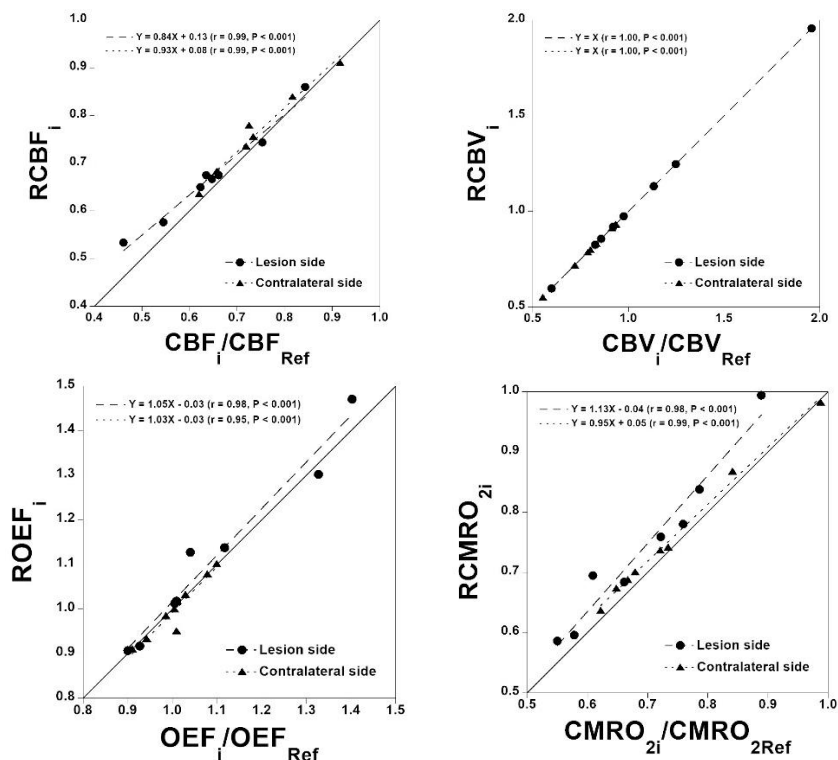


Figure 3. The relation between the ratio of CBF_i to CBF_{Ref} obtained by the steady-state method with arterial blood sampling and $RCBF_i$ calculated by the present method for both the cerebral lesion and the contralateral side of the cerebral lesion (A). Such relations for $RCBV_i$, $ROEF_i$, and $RCMRO_{2i}$ are also shown (B, C, and D, respectively)

The simulation of relations between assumed $RCBF_i$ and estimated $RCBF_i$ when CBF_{Ref} deviates from the assumed value is shown in Figure 4A. The simulation of errors in estimated

$RCBF_i$ for assumed $RCBF_i$ is also shown in Figure 4B. Errors in estimated $RCBF_i$ were within $\pm 10\%$ when assumed $RCBF_i$ varied from 0.4 to 1.0.

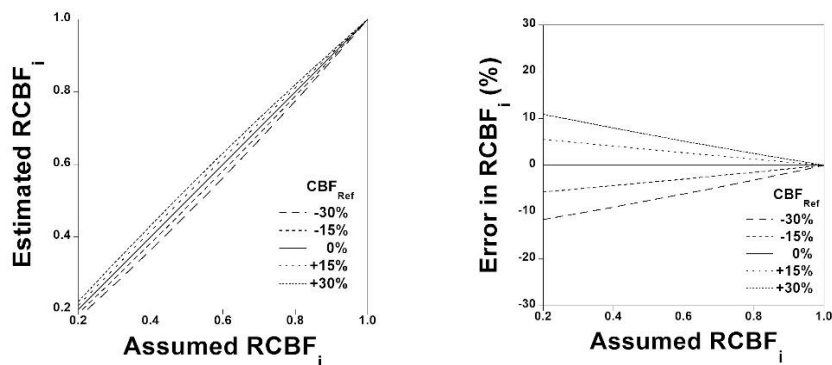


Figure 4. Simulation of relation between the assumed $RCBF_i$ and estimated $RCBF_i$ when CBF_{Ref} deviates from the assumed value (A). Simulation of errors in the estimated $RCBF_i$ for assumed $RCBF_i$ (B)

The simulation of relations between assumed $ROEF_i$ and estimated $ROEF_i$ when CBF_{Ref} deviates from the assumed value is shown in Figure 5A, 5B, and 5C for $RCBV_i$ of 1.0, 1.5, and 2.0, respectively. The simulation of errors in

estimated $ROEF_i$ for assumed $ROEF_i$ is also shown in Figure 6A, 6B, and 6C for $RCBV_i$ of 1.0, 1.5, and 2.0, respectively. Errors in estimated $ROEF_i$ were within $\pm 5\%$ when assumed $ROEF_i$ varied from 1.0 to 1.5.

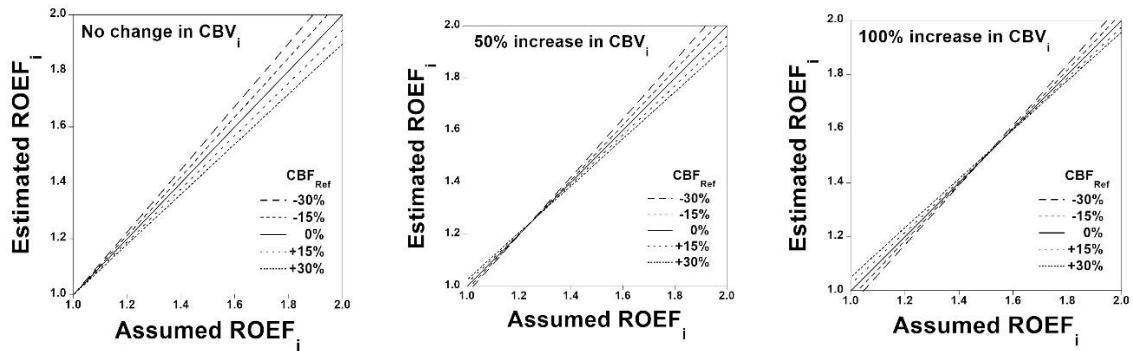


Figure 5. Simulation of relation between the assumed $ROEF_i$ and estimated $ROEF_i$ when CBF_{Ref} deviates from the assumed value for $RCBV_i$ of 1.0, 1.5, and 2.0 (A, B, and C, respectively)

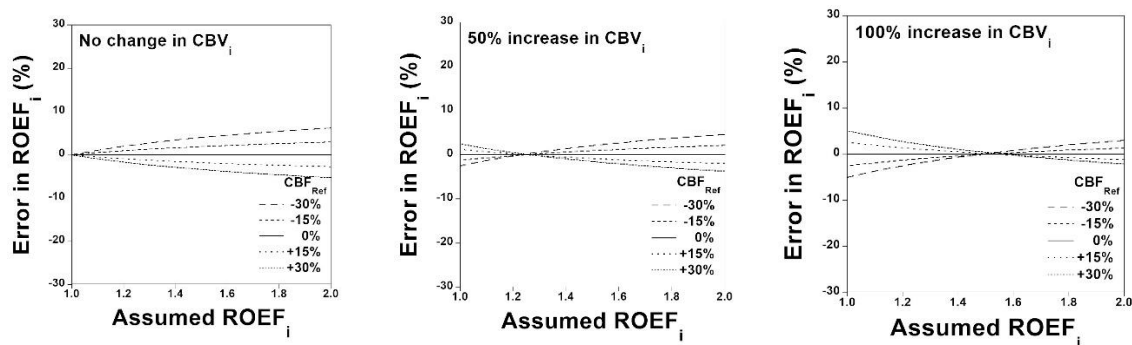


Figure 6. Simulation of errors in the estimated $ROEF_i$ for assumed $ROEF_i$ for $RCBV_i$ of 1.0, 1.5, and 2.0 (A, B, and C, respectively)

The simulation of relations between assumed $RCMRO_{2i}$ and estimated $RCMRO_{2i}$ when CBF_{Ref} deviates from the assumed value is shown in Figure 7A. The simulation of errors in estimated

$RCMRO_{2i}$ for assumed $RCMRO_{2i}$ is also shown in Figure 7B. Errors in estimated $RCMRO_{2i}$ were within $\pm 10\%$ when assumed $RCMRO_{2i}$ varied from 0.4 to 1.0.

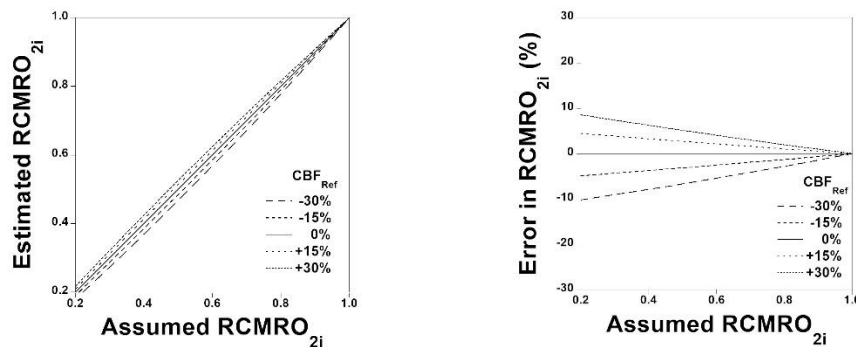


Figure 7. Simulation of relation between the assumed $RCMRO_{2i}$ and estimated $RCMRO_{2i}$ when CBF_{Ref} deviates from the assumed value (A). Simulation of errors in the estimated $RCMRO_{2i}$ for assumed $RCMRO_{2i}$ (B)

Discussion

The measurement of CBF, CBV, OEF, and $CMRO_2$ using PET and oxygen-15 labeled gases is widely used to investigate the pathophysiology of occlusive cerebrovascular disease (1-8). The steady-state method for quantification of CBF, CBV, OEF, and $CMRO_2$ is a method that has been commonly used for a long time (17, 18, 22). However, this method requires invasive arterial blood sampling. Therefore, we have developed a method for

quantification of CBF, CBV, OEF, and $CMRO_2$ without invasive arterial blood sampling based on the steady-state method which is simple in PET examination procedure and needs the long PET examination time as compared with other various acquisition protocols.

In the present study, good correlations were observed for $RCBF_i$, $RCBV_i$, $ROEF_i$, and $RCMRO_{2i}$ calculated by the present method compared with those obtained by the steady-state method with arterial blood sampling for

both the cerebral lesions of occlusive cerebrovascular diseases and the contralateral side of cerebral lesions. The simulation showed that errors in estimated $RCBF_i$ were within $\pm 10\%$ when assumed $RCBF_i$ varied from 0.4 to 1.0. These results indicate the validity of the present method.

The stage II hemodynamic change in occlusive cerebrovascular diseases, so-called "misery perfusion", due to decreased cerebral perfusion pressure below the lower limit of cerebral autoregulation shows a decrease in CBF with an increase in OEF for maintenance of $CMRO_2$ and with an increase in CBV (2). In the simulation studies, errors in estimated $ROEF_i$ were within $\pm 5\%$ when assumed $ROEF_i$ varied from 1.0 to 1.5 for $RCBV_i$ of 1.0 to 2.0, indicating the validity of the present method in the condition of misery perfusion. To estimate OEF, an indicator of stage II hemodynamic change, some non-invasive methods have been developed that used PET scanning data with ^{15}O -labeled water and $^{15}O_2$ gas but without $C^{15}O$ gas (19, 20). However, increased CBV in stage II hemodynamic change might cause non-negligible OEF estimation errors (20). In the present method, $RCBV_i$ was also estimated using PET scanning data with $C^{15}O$ gas; therefore, errors in estimated $ROEF_i$ were negligibly small.

Oxygen hypometabolism with hypoperfusion in occlusive cerebrovascular diseases, so-called "matched hypoperfusion", showing decreases in CBF and $CMRO_2$ can be observed in lesions with neural damage (32). In the simulation studies, errors in estimated $RCMRO_{2i}$ were within $\pm 10\%$ when assumed $RCMRO_{2i}$ varied from 0.4 to 1.0, indicating the validity of the present method in the condition of matched hypoperfusion.

Good correlations were observed for $RCBF_i$, $RCBV_i$, $ROEF_i$, and $RCMRO_{2i}$ calculated by the present method compared to those obtained by the steady-state method with arterial blood sampling. Simulation studies showed that errors in estimated $RCBF_i$, $ROEF_i$, and $RCMRO_{2i}$ were negligibly small. However, a limitation of this study is the small number of patients ($n=8$). The present method should be validated with large series of patients in a multicenter study with various PET scanners and reconstruction methods.

Conclusion

A simple method for quantification of CBF, CBV, OEF, and $CMRO_2$ using PET and three oxygen-15 labeled gases, $C^{15}O_2$, $C^{15}O$, and $^{15}O_2$, without invasive arterial blood sampling has been developed based on the steady-state method. Good correlations were observed for $RCBF_i$,

$RCBV_i$, $ROEF_i$, and $RCMRO_{2i}$ calculated by the present method compared with those obtained by the steady-state method with arterial blood sampling, indicating its validity. Simulation studies showed that errors in estimated $RCBF_i$, $ROEF_i$, and $RCMRO_{2i}$ were negligibly small for both conditions of misery perfusion and matched hypoperfusion. The present method can be used to investigate the pathophysiology of occlusive cerebrovascular disease.

Acknowledgments

We thank Mr. Minoru Oto, Ms. Yayoi Kurihara and Mr. Katsuyuki Kikori for their assistance in the PET experiments.

Conflict of interest

The authors declare that they have no conflict of interest.

Funding

This study was supported in part by a Grant-in-Aid for Scientific Research (C) (No. 20K08031) from the Japan Society for the Promotion of Science.

Author's contribution

HI, MI, RY, HK, and KT contributed to the design of the study. HI, RY, NU, SI, HK, and KT performed the PET measurements. NU, HK, and KT performed the image reconstruction and the calculation of parametric images. HI, MI, RY, NU, and SI performed the data analyses. HI, MI, RY, NU, SI, and KF contributed to the interpretation of the data. HI and MI wrote the manuscript.

References

1. Gibbs JM, Wise RJ, Leenders KL, Jones T. Evaluation of cerebral perfusion reserve in patients with carotid-artery occlusion. *Lancet*. 1984; 1(8372): 310-4.
2. Powers WJ, Grubb RL, Raichle ME. Physiological responses to focal cerebral ischemia in humans. *Ann Neurol*. 1984; 16(5): 546-52.
3. Powers WJ, Grubb RL, Darriet D, Raichle ME. Cerebral blood flow and cerebral metabolic rate of oxygen requirements for cerebral function and viability in humans. *J Cereb Blood Flow Metab*. 1985; 5(4): 600-8.
4. Leblanc R, Yamamoto YL, Tyler JL, Diksic M, Hakim A. Borderzone ischemia. *Ann Neurol*. 1987; 22(6):707-13.
5. Kanno I, Uemura K, Higano S, Murakami M, Iida H, Miura S, et al. Oxygen extraction fraction at maximally vasodilated tissue in the ischemic brain estimated from the regional CO_2 responsiveness measured by

- positron emission tomography. *J Cereb Blood Flow Metab.* 1988; 8(2): 227-35.
6. Sette G, Baron JC, Mazoyer B, Levasseur M, Pappata S, Crouzel C. Local brain haemodynamics and oxygen metabolism in cerebrovascular disease. Positron emission tomography. *Brain.* 1989; 112(Pt 4): 931-51.
 7. Yamauchi H, Fukuyama H, Kimura J, Konishi J, Kameyama M. Hemodynamics in internal carotid artery occlusion examined by positron emission tomography. *Stroke.* 1990; 21(10):1400-6.
 8. Okazawa H, Kudo T. Clinical impact of hemodynamic parameter measurement for cerebrovascular disease using positron emission tomography and ^{15}O -labeled tracers. *Ann Nucl Med.* 2009; 23(3): 217-27.
 9. Ogasawara K, Ito H, Sasoh M, Okuguchi T, Kobayashi M, Yukawa H, et al. Quantitative measurement of regional cerebrovascular reactivity to acetazolamide using ^{123}I -N-isopropyl-p-iodoamphetamine autoradiography with SPECT: validation study using H_2^{15}O with PET. *J Nucl Med.* 2003; 44(4): 520-5.
 10. Ito H, Inoue K, Goto R, Kinomura S, Sato T, Kaneta T, et al. Error analysis of measured cerebral vascular response to acetazolamide stress by I-123-IMP autoradiographic method with single photon emission computed tomography: errors due to distribution volume of I-123-IMP. *Ann Nucl Med.* 2004; 18(3): 221-6.
 11. Derdeyn CP, Grubb RL, Jr., Powers WJ. Cerebral hemodynamic impairment: methods of measurement and association with stroke risk. *Neurology.* 1999; 53(2): 251-9.
 12. Everett BA, Oquendo MA, Abi-Dargham A, Nobler MS, Devanand DP, Lisanby SH, et al. Safety of radial arterial catheterization in PET research subjects. *J Nucl Med.* 2009; 50(10): 1742.
 13. Iguchi S, Hori Y, Moriguchi T, Morita N, Yamamoto A, Koshino K, et al. Verification of a semi-automated MRI-guided technique for non-invasive determination of the arterial input function in ^{15}O -labeled gaseous PET. *Nucl Instrum Methods Phys Res A.* 2013; 702: 111-3.
 14. Su Y, Vlassenko AG, Couture LE, Benzinger TL, Snyder AZ, Derdeyn CP, et al. Quantitative hemodynamic PET imaging using image-derived arterial input function and a PET/MR hybrid scanner. *J Cereb Blood Flow Metab.* 2017; 37(4): 1435-46.
 15. Kudomi N, Maeda Y, Yamamoto H, Yamamoto Y, Hatakeyama T, Nishiyama Y. Reconstruction of input functions from a dynamic PET image with sequential administration of $^{15}\text{O}_2$ and [Formula: see text] for noninvasive and ultra-rapid measurement of CBF, OEF, and CMRO_2 . *J Cereb Blood Flow Metab.* 2018; 38(5): 780-92.
 16. Van der Weijden CWJ, Mossel P, Bartels AL, Dierckx R, Luurtsema G, Lammertsma AA, et al. Non-invasive kinetic modelling approaches for quantitative analysis of brain PET studies. *Eur J Nucl Med Mol Imaging.* 2023; 50(6): 1636-50.
 17. Frackowiak RS, Lenzi GL, Jones T, Heather JD. Quantitative measurement of regional cerebral blood flow and oxygen metabolism in man using ^{15}O and positron emission tomography: theory, procedure, and normal values. *J Comput Assist Tomogr.* 1980; 4(6): 727-36.
 18. Ito H, Kanno I, Kato C, Sasaki T, Ishii K, Ouchi Y, et al. Database of normal human cerebral blood flow, cerebral blood volume, cerebral oxygen extraction fraction and cerebral metabolic rate of oxygen measured by positron emission tomography with ^{15}O -labelled carbon dioxide or water, carbon monoxide and oxygen: a multicentre study in Japan. *Eur J Nucl Med Mol Imaging.* 2004; 31(5): 635-43.
 19. Derdeyn CP, Videen TO, Simmons NR, Yundt KD, Fritsch SM, Grubb RL, Jr., et al. Count-based PET method for predicting ischemic stroke in patients with symptomatic carotid arterial occlusion. *Radiology.* 1999; 212(2): 499-506.
 20. Ibaraki M, Shimosegawa E, Miura S, Takahashi K, Ito H, Kanno I, et al. PET measurements of CBF, OEF, and CMRO_2 without arterial sampling in hyperacute ischemic stroke: method and error analysis. *Ann Nucl Med.* 2004; 18(1): 35-44.
 21. Kobayashi M, Okazawa H, Tsuchida T, Kawai K, Fujibayashi Y, Yonekura Y. Diagnosis of misery perfusion using noninvasive ^{15}O -gas PET. *J Nucl Med.* 2006; 47(10): 1581-6.
 22. Ito H, Kubo H, Takahashi K, Nishijima KI, Ukon N, Nemoto A, et al. Integrated PET/MRI scanner with oxygen-15 labeled gases for quantification of cerebral blood flow, cerebral blood volume, cerebral oxygen extraction fraction and cerebral metabolic rate of oxygen. *Ann Nucl Med.* 2021; 35(4): 421-8.
 23. Phelps ME, Huang SC, Hoffman EJ, Kuhl DE. Validation of tomographic measurement of cerebral blood volume with C-11-labeled carboxyhemoglobin. *J Nucl Med.* 1979; 20(4): 328-34.
 24. Martin WR, Powers WJ, Raichle ME. Cerebral blood volume measured with inhaled C^{15}O

- and positron emission tomography. *J Cereb Blood Flow Metab.* 1987; 7(4): 421-6.
25. Iida H, Jones T, Miura S. Modeling approach to eliminate the need to separate arterial plasma in oxygen-15 inhalation positron emission tomography. *J Nucl Med.* 1993; 34(8): 1333-40.
 26. Lammertsma AA, Jones T. Correction for the presence of intravascular oxygen-15 in the steady-state technique for measuring regional oxygen extraction ratio in the brain: 1. description of the method. *J Cereb Blood Flow Metab.* 1983; 3(4): 416-24.
 27. Lammertsma AA, Baron JC, Jones T. Correction for intravascular activity in the oxygen-15 steady-state technique is independent of the regional hematocrit. *J Cereb Blood Flow Metab.* 1987; 7(3): 372-4.
 28. Delso G, Furst S, Jakoby B, Ladebeck R, Ganter C, Nekolla SG, et al. Performance measurements of the Siemens mMR integrated whole-body PET/MR scanner. *J Nucl Med.* 2011; 52(12): 1914-22.
 29. Watson CC, Newport D, Casey ME. A single scatter simulation technique for scatter correction in 3D PET. In: Grangeat P, Amans JL, editors. *Three-dimensional image reconstruction in radiology and nuclear medicine.* Dordrecht, the Netherlands: Kluwer Academic Publishers; 1996. p. 255-68.
 30. Burnett RW, Noonan DC. Calculations and correction factors used in determination of blood pH and blood gases. *Clin Chem.* 1974; 20(12): 1499-506.
 31. Dickson JC, O'Meara C, Barnes A. A comparison of CT- and MR-based attenuation correction in neurological PET. *Eur J Nucl Med Mol Imaging.* 2014; 41(6): 1176-89.
 32. Kuroda S, Shiga T, Ishikawa T, Houkin K, Narita T, Katoh C, et al. Reduced blood flow and preserved vasoreactivity characterize oxygen hypometabolism due to incomplete infarction in occlusive carotid artery diseases. *J Nucl Med.* 2004; 45(6): 943-9.
 33. Ito H, Kanno I, Shimosegawa E, Tamura H, Okane K, Hatazawa J. Hemodynamic changes during neural deactivation in human brain: a positron emission tomography study of crossed cerebellar diaschisis. *Ann Nucl Med.* 2002; 16(4): 249-54.

Appendix

The theory of the steady-state method for quantification of CBF, CBV, OEF, and CMRO₂ using PET and oxygen-15 labeled gases is as

follows (17). CBF, CBV, OEF, and CMRO₂ in a brain region are defined as CBF_i , CBV_i , OEF_i , and $CMRO_{2i}$. The radioactivity concentrations in the brain and blood are defined as follows:

$C_i^{CO_2}$: Radioactivity concentration of H₂¹⁵O in a brain region measured by PET during inhalation of C¹⁵O₂ gas after equilibrium had been reached

C_i^{CO} : Radioactivity concentration of hemoglobin (Hb)C¹⁵O in a brain region measured by PET after inhalation of C¹⁵O gas

$C_i^{O_2}$: Radioactivity concentration in a brain region measured by PET during inhalation of ¹⁵O₂ gas after equilibrium had been reached

$C_a^{CO_2}$: Radioactivity concentration of H₂¹⁵O in whole blood during inhalation of C¹⁵O₂ gas after equilibrium had been reached

$C_p^{CO_2}$: Radioactivity concentration of H₂¹⁵O in plasma during inhalation of C¹⁵O₂ gas after equilibrium had been reached

C_a^{CO} : Radioactivity concentration of HbC¹⁵O in whole blood after inhalation of C¹⁵O gas

$C_a^{O_2}$: Radioactivity concentration in whole blood during inhalation of ¹⁵O₂ gas after equilibrium had been reached

$C_{a[O_2]}^{O_2}$: Radioactivity concentration of Hb¹⁵O₂ in whole blood during inhalation of ¹⁵O₂ gas after equilibrium had been reached

$C_{a[w]}^{O_2}$: Radioactivity concentration of H₂¹⁵O in whole blood during inhalation of ¹⁵O₂ gas after equilibrium had been reached

$C_{p[w]}^{O_2}$: Radioactivity concentration of H₂¹⁵O in plasma during inhalation of ¹⁵O₂ gas after equilibrium had been reached

1. Inhalation of C¹⁵O₂ gas

C¹⁵O₂ is converted to H₂¹⁵O in the lung. Time derivative of radioactivity concentration of H₂¹⁵O in a brain region, $\frac{dC_i^{CO_2}}{dt}$ can be expressed as follows:

$$\frac{dC_i^{CO_2}}{dt} = E \cdot CBF_i \cdot C_a^{CO_2} - \frac{E \cdot CBF_i}{p} C_i^{CO_2} - \lambda C_i^{CO_2} \quad \text{Eq. A1}$$

Where E is the first-pass extraction fraction of H₂¹⁵O in the brain, which can be assumed to be unity. p is the brain-blood partition coefficient, which can be assumed to be unity. λ is the decay constant of ¹⁵O. Since $\frac{dC_i^{CO_2}}{dt} = 0$ during equilibrium condition, the following equations are derived from Eq. A1:

$$C_i^{CO_2} = \frac{CBF_i \cdot C_a^{CO_2}}{\frac{CBF_i}{p} + \lambda} \quad \text{Eq. A2}$$

$$CBF_i = \frac{\lambda}{\frac{C_a^{CO_2}}{C_i^{CO_2}} - \frac{1}{p}} \quad \text{Eq. A3}$$

2. Inhalation of $C^{15}O$ gas

$C^{15}O$ binds to hemoglobin ($HbC^{15}O$) after inhalation. C_i^{CO} can be expressed as follows (23, 24):

$$C_i^{CO} = CBV_i \cdot C_a^{CO} \frac{h}{H} \quad \text{Eq. A4}$$

Where h and H are hematocrits in the cerebral vessel and the large vessel, respectively. The hematocrit ratio of cerebral to large vessels, $\frac{h}{H}$ can be assumed to be 0.85. The following equation is derived from Eq. A4:

$$CBV_i = \frac{\frac{C_i^{CO}}{C_a^{CO}}}{\frac{h}{H}} \quad \text{Eq. A5}$$

3. Inhalation of $^{15}O_2$ gas

$^{15}O_2$ binds to hemoglobin ($Hb^{15}O_2$) after inhalation. ^{15}O -labeled water is produced from aerobic metabolism using $^{15}O_2$ in the brain, which is called metabolic water ($H_2^{15}Om$). Recirculating ^{15}O -labeled water ($H_2^{15}Or$) resulting from washout of metabolic water from body tissues, including the brain, is supplied to the brain depending on CBF_i . $C_i^{O_2}$ is equal to the sum of radioactivity concentration of $H_2^{15}Om$ in a brain region ($C_{im}^{O_2}$) and radioactivity concentration of $H_2^{15}Or$ in a brain region ($C_{ir}^{O_2}$).

$$C_i^{O_2} = C_{im}^{O_2} + C_{ir}^{O_2} \quad \text{Eq. A6}$$

$C_{im}^{O_2}$ and $C_{ir}^{O_2}$ can be expressed as follows:

$$C_{im}^{O_2} = \frac{C_{a[o]}^{O_2} \cdot CBF_i \cdot OEF'_i}{\frac{CBF_i}{p} + \lambda} \quad \text{Eq. A7}$$

$$C_{ir}^{O_2} = \frac{C_{a[w]}^{O_2} \cdot CBF_i}{\frac{CBF_i}{p} + \lambda} \quad \text{Eq. A8}$$

Where OEF'_i is cerebral oxygen extraction fraction without correction of remaining radioactivity concentration of $^{15}O_2$ in the cerebral vessels (26, 27). From Eq. A2, A3, A7 and A8 OEF'_i can be expressed as follows:

$$OEF'_i = \frac{C_a^{CO_2}}{C_{a[o]}^{CO_2}} \left(\frac{C_i^{O_2}}{C_i^{CO_2}} - \frac{C_{a[w]}^{O_2}}{C_a^{CO_2}} \right) \quad \text{Eq. A9}$$

Since the ratio of $C_a^{CO_2}$ to $C_p^{CO_2}$ is equal to the ratio of $C_{a[w]}^{O_2}$ to $C_{p[w]}^{O_2}$, $C_{a[w]}^{O_2}$ can be expressed as follows:

$$C_{a[w]}^{O_2} = \frac{C_a^{CO_2}}{C_p^{CO_2}} C_{p[w]}^{O_2} \quad \text{Eq. A10}$$

$C_p^{CO_2}$ and $C_{p[w]}^{O_2}$ can be obtained by plasma separation of arterial blood samples during inhalation of $C^{15}O_2$ gas after equilibrium had been reached and during inhalation of $^{15}O_2$ gas after equilibrium had been reached, respectively. $C_{a[o]}^{O_2}$ can be obtained from following equation:

$$C_a^{O_2} = C_{a[o]}^{O_2} + C_{a[w]}^{O_2} \quad \text{Eq. A11}$$

From Eq. A9, A10, and A11, OEF'_i can be expressed as follows:

$$OEF'_i = \frac{\frac{C_i^{O_2}}{C_i^{CO_2}} \frac{C_a^{CO_2}}{C_{p[w]}^{O_2}} - \frac{C_a^{CO_2}}{C_p^{CO_2}}}{\frac{C_a^{O_2}}{C_{p[w]}^{O_2}} - \frac{C_a^{CO_2}}{C_p^{CO_2}}} \quad \text{Eq. A12}$$

In measurement of cerebral oxygen extraction fraction, effects of remaining radioactivity concentration of $^{15}O_2$ in the cerebral vessels should be corrected (26, 27). The cerebral oxygen extraction fraction with correction of remaining radioactivity concentration of $^{15}O_2$ in the cerebral vessels, OEF_i , can be expressed as follows:

$$OEF_i = \frac{OEF'_i - X_i}{1 - X_i} \quad \text{Eq. A13}$$

Where

$$X_i = \frac{\frac{CBF_i}{p} + \lambda}{\frac{h}{H} CBF_i} \quad \text{Eq. A14}$$

$CMRO_{2i}$ can be expressed as follows:

$$CMRO_{2i} = OEF_i \cdot CBF_i \cdot [O_2] \quad \text{Eq. A15}$$

Where $[O_2]$ is the total oxygen content in arterial blood which can be estimated from P_aO_2 , pH and Hb concentration (18, 30).